



Article

An Integrated Analysis of the Eutrophication Process in the Enxoé Reservoir within the DPSIR Framework

Tiago B. Ramos ^{1,*} , Hanaa Darouich ², Maria C. Gonçalves ³, David Brito ¹, Maria A. Castelo Branco ³, José C. Martins ³, Manuel L. Fernandes ³, Fernando P. Pires ³, Manuela Morais ⁴  and Ramiro Neves ¹

¹ Centro de Ciência e Tecnologia do Ambiente e do Mar (MARETEC), Instituto Superior Técnico, Universidade de Lisboa, Av. Rovisco Pais, 1, 1049-001 Lisboa, Portugal; odavidbrito@gmail.com (D.B.); ramiro.neves@tecnico.ulisboa.pt (R.N.)

² Centro de Investigação em Agronomia, Alimentos, Ambiente e Paisagem (LEAF), Instituto Superior de Agronomia, Universidade de Lisboa, Tapada da Ajuda, 1349-017 Lisboa, Portugal; hanaa.darouich@gmail.com

³ Instituto Nacional de Investigação Agrária e Veterinária (INIAV), Quinta do Marquês, Av. República, 2784-505 Oeiras, Portugal; maria.goncalves@iniav.pt (M.C.G.); amelia.castelobranco@iniav.pt (M.A.C.B.); j.casimiro@iniav.pt (J.C.M.); Manuel.fernandes@iniav.pt (M.L.F.); fernando.pires@iniav.pt (F.P.P.)

⁴ Department of Biology, Institute of Earth Sciences (ICT), University of Évora, Largo dos Colegiais, 7000 Évora, Portugal; mmorais@uevora.pt

* Correspondence: tiagobramos@tecnico.ulisboa.pt; Tel.: +35-121-841-9428

Received: 10 October 2018; Accepted: 2 November 2018; Published: 4 November 2018



Abstract: The Enxoé reservoir in southern Portugal has been exhibiting the highest trophic state in the country since its early years of operation. The problem has attracted water managers' and researchers' attention as the reservoir is the water supply for two municipalities. Extensive research was thus conducted over the last few years, including field monitoring and modelling at the plot, catchment, and reservoir scales. This study now frames all partial findings within the Driver-Pressure-State-Impact-Response (DPSIR) framework to better understand the eutrophication process in the Enxoé reservoir. Agriculture and grazing were found to have a reduced role in the eutrophication of the reservoir, with annual sediment and nutrient loads being comparably smaller or similar to those reported for other Mediterranean catchments. Flash floods were the main mechanism for transporting particle elements to the reservoir, being in some cases able to carry up three times the average annual load. However, the main eutrophication mechanisms in the reservoir were P release from deposited sediment under anoxic conditions and the process of internal recycling of organic matter and nutrients. Reducing the P load from the catchment and deposited sediment could lead to a mesotrophic state level in the reservoir. However, this level would only be sustainable by limiting the P internal load ability to reach the photic zone.

Keywords: catchment; eutrophication; modelling; nutrients; trophic level.

1. Introduction

Agriculture is commonly pointed out as the major contributor for surface water eutrophication, with inefficient practices resulting in high nutrient surpluses (particularly phosphorus (P) and nitrogen (N)) that are transferred to water bodies through diffuse processes (runoff and leaching), promoting algae blooms, oxygen depletion and biodiversity loss. In this matter, P is usually considered the single most limiting nutrient for phytoplankton growth, namely cyanobacteria. Although P losses from agricultural land are normally low ($0.1\text{--}6\text{ kg ha}^{-1}$) when compared to fertilization inputs [1], such values may have a significant impact on aquatic ecosystems. However, the link between agriculture

and water quality problems observed downstream cannot be automatically established as each system is unique and the precise role of agriculture in eutrophication remains poorly understood. As result, numerous research studies have been performed to define the best adaptative measures to counteract an environmental problem that remains a major concern worldwide [2–13].

Lake reservoirs are particularly vulnerable to eutrophication, with increasing nutrient loading from upstream catchments promoting the development of primary producers (phytoplankton, cyanobacteria, aquatic plants), conditions of hypoxia and anoxia and biodiversity loss. Lake vulnerability to eutrophication has been associated with its hydrological (catchment land use, inflows) and morphometric (volume, depth) characteristics [14]. Also, the low water velocities registered in reservoirs, their high residence time and the existence of thermal stratification help promoting the two main processes that drive N and P biogeochemical cycles: the primary production and the settling of particulate matter [14–16].

The Enxoé reservoir located in southern Portugal is a representative example of the need for better understanding the relationship between agriculture and the quality of downstream water bodies. The Enxoé reservoir has been displaying the highest eutrophic state in the country since its early years of operation (2000). Frequent chlorophyll-a blooms have been registered since then, with cyanobacteria being also reported during the spring and summer seasons [17–19]. Such conditions pose a serious problem for water managers as the reservoir is the water supply for two municipalities (Serpa and Mértola) and extensive water treatment is always required.

Understanding the eutrophic condition of the Enxoé reservoir has quickly drawn researchers' attention as extensive agriculture practices and grazing carried out upstream could not alone explain the frequent algae blooms observed. Coelho and Leitão [20] proposed a first explanation for such high eutrophic state. These authors suggested a link between cyanobacterial blooms and nutrient input loads from the catchment, particularly P, which would fuel a process of both a fast and a delayed response in the reservoir. The consumption of input dissolved nutrients would trigger initial algae blooms, while sediment sources would be responsible for later blooms. However, a more comprehensive analysis was necessary to better understand the main physical and biochemical processes involved in the eutrophication process of the reservoir since the catchment was ungauged and detailed monitoring was needed.

Hence, Ramos et al. [21,22] conducted detailed hydro-biogeochemical monitoring of suspended sediment (SSC) and nutrient concentrations, including P (in both particulate and soluble forms), nitrate (NO_3^-) and organic carbon (also in both particulate (POC) and soluble (DOC) forms)), in the Enxoé River during three hydrological years (2010–2013), estimating loads to the reservoir and further identifying the main source areas in the catchment. These studies showed the strong seasonal and annual variability of sediment and nutrient dynamics in the catchment, highlighting the role of flash floods in the transport of sediment and particulate nutrients. Brito et al. [23,24] modelled then sediment and nutrient long-term dynamics in the catchment and the contribution of flood events to the reservoir total loads. Also, Rodrigues et al. [25] mapped soil erosion risks in the catchment using the PESERA model [26]. On the other hand, Morais et al. [19] monitored physical, chemical and phytoplankton parameters in the Enxoé reservoir for three years (2010–2012) to evaluate the state of the reservoir. Finally, Brito et al. [27] simulated the actual reservoir state and depicted the origin of the Enxoé's reservoir trophic status using the CE-QUAL-W2 model [28].

This study now aims to integrate all previous research within the Driver-Pressure-State-Impact-Response (DPSIR) framework [29] as well as additional data obtained during several research projects carried out in the Enxoé region over the last few years. The DPSIR framework establishes a chain of causal links between the socioeconomic factors (drivers), forcing anthropogenic activities (pressures), the resulting environmental conditions (state), the environmental consequences resulting from these conditions (impacts) and finally, the measures that need to be taken to improve the environmental state (response). It has been widely considered as a valuable tool for defining sustainable and environmentally friendly measures to improve water management policies at the catchment

scale [30–33]. Tscherning et al. [34] further considered it as a useful tool for providing policy makers with meaningful explanations of cause and effect relationships, contributing for bridging the gap between policy makers and stakeholders. In this study, the DPSIR framework is applied to (i) to better understand the role of agriculture in the eutrophication of the Enxoé reservoir; (ii) to depict the processes involved in the remobilization of P at different scales; (iii) to quantify their importance for water quality in the reservoir; and (iv) to propose mitigation measures to improve the trophic state of the reservoir, reducing the frequency and the intensity of algae blooms.

2. Materials and Methods

2.1. Study Area

The Enxoé catchment is in the Alentejo region, southern Portugal (Figure 1). The river is a tributary of the Guadiana River, has a catchment area of 60.8 km² and a bed length of 9 km. The altitude ranges from 155 to 348 m. The main soil reference groups are Luvisols (in 47% of the area), Cambisols (31%) and Calcisols (14%). Olive orchards (18.3 km²), agro-forestry of holm oaks (17.6 km²) and annual winter crops (17.0 km²) are the main land uses. The annual mean surface air temperature reaches 16 °C, while the annual reference evapotranspiration (ET₀) ranges from 1200 to 1300 mm. The mean annual precipitation is 500 mm, presenting strong seasonal (80% is concentrated between October and April) and intra-annual variability. As a result, the precipitation regime varies between relatively abundant rainfall events that occur in only a few minutes or hours and frequent drought episodes that can last from a few months to a couple of years. Hence, the river discharge also exhibits strong inter and intra-annual variation. High flow discharges are observed after storm events from fall to spring while there is no flow during the summer season. The Enxoé River then forms over the annual cycle small lentic shallow systems where sediment and nutrients accumulate followed by lotic systems where high flushing rates are often observed.

The catchment has a population of 1000 inhabitants, mostly located in Vale de Vargo. The Enxoé reservoir, build in 2000, limits the study area downstream. The reservoir has a volume of 10.4 hm³, a surface area close to 2 km² and average and maximum depths of 5 and 17 m, respectively. The reservoir supplies the villages of Serpa and Mértola (25,000 inhabitants) located outside the catchment area. There are no point source emissions in Enxoé as waste waters from the treatment plant of Vale de Vargo are pumped to a water stream located outside the catchment.

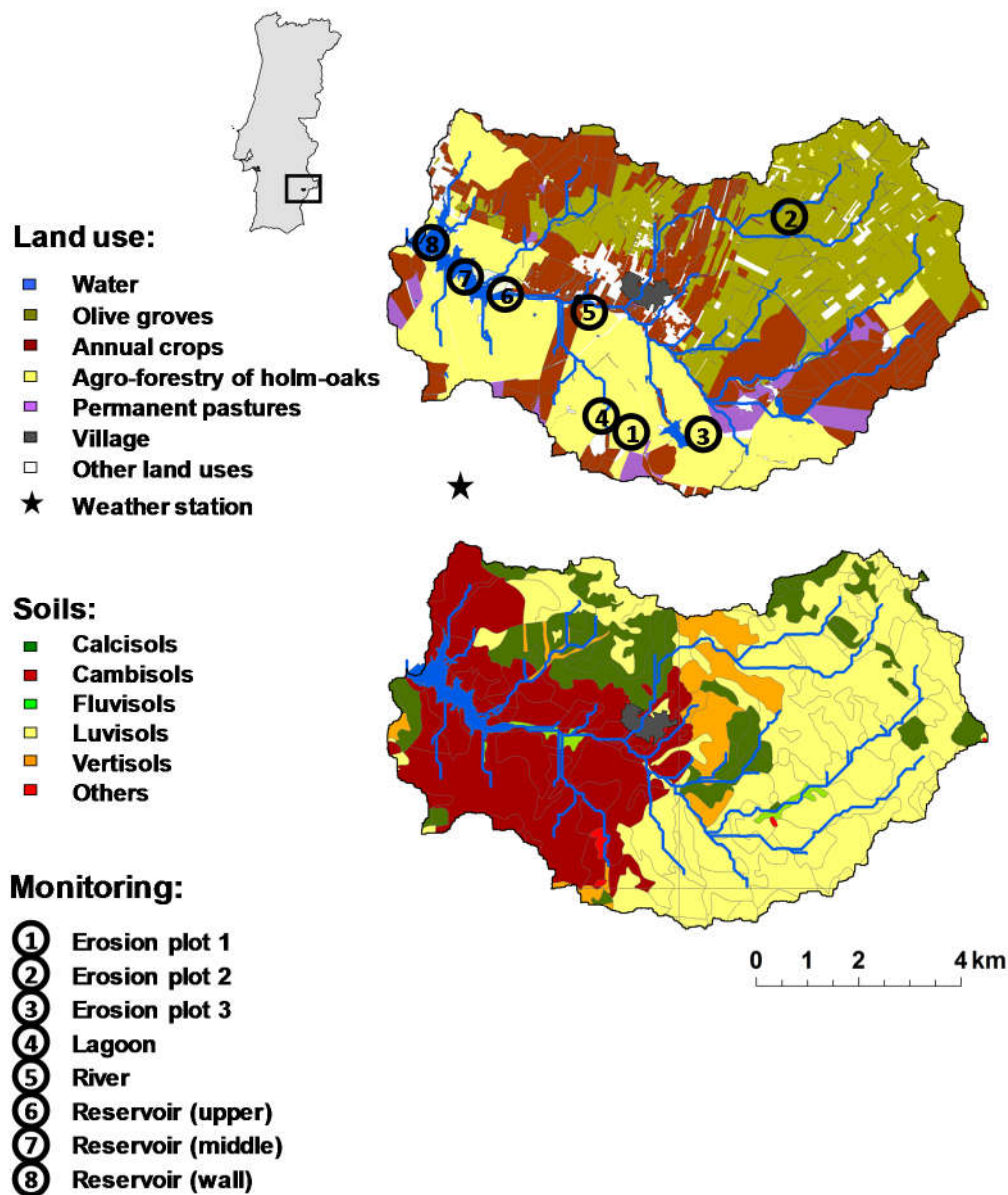


Figure 1. Location, land use (top) and major soil units (bottom) in Enxoé.

2.2. Data Collection

2.2.1. Field Plots

Soil erosion was monitored in 3 field plots between October 2009 and April 2013:

- Plot 1, with 800 m² (37°57'42" N; 7°25'11" W), was in an agro-forestry of holm oaks area, which included oats for grazing. The soil was a Cambisol with loamy sand texture derived from granite;
- Plot 2, with 180 m² (37°56'32" N; 7°26'36" W), was in an olive grove with no soil cover between crop rows. The soil was a Cambisol with clay loam texture derived from calcareous rock;
- Plot 3, with 380 m² (37°57'25" N; 7°23'59" W), was in an agro-forestry of holm oaks area under fallow. The soil was a Luvisol with loamy texture derived from schist.

In each plot, runoff and associated sediment were collected using V shaped metal sheet barriers. The vertices were connected to the storage containers, consisting of three tanks located at the base of each plot. Total runoff and soil losses were measured after each erosion event (i.e., an event producing measurable runoff) or, occasionally, after a series of events if they were separated by a short time

interval. Runoff was determined from the volume of water collected in the storage containers. Runoff water (water and sediment) was thoroughly mixed and samples were collected to determine SSC, total phosphorus (TP), particulate phosphorus (PP) consisting of P adsorbed to particulate ($>0.45\ \mu\text{m}$) suspended material, soluble reactive phosphorus (SRP), NO_3^- , POC, DOC, electrical conductivity (EC), major cations (Ca^{2+} , Mg^{2+} , K^+ and Na^+), total iron (Fe) and pH. Laboratory methodologies used for characterizing the water samples can be found in Ramos et al. [21,22].

2.2.2. Lagoon

The water quality of a small lagoon draining $0.045\ \text{km}^2$ was also monitored between January 2010 and April 2013 ($37^\circ 57' 51''\ \text{N}$; $7^\circ 25' 19''\ \text{W}$). Sampling was for the same elements monitored in the erosion plots. Soil and land cover characteristics in the drainage area were the same as in erosion Plot 1.

2.2.3. Enxoé River

The Enxoé River water was monitored at a sampling station located at the outlet of the catchment before the reservoir ($37^\circ 58' 47''\ \text{N}$; $7^\circ 24' 60''\ \text{W}$) from September 2010 to August 2013, covering a drainage area close to $45\ \text{km}^2$ (Figure 1). The water stream level and turbidity were measured using an YSI 6920 measuring probe (YSI Incorporated, Yellow Springs, OH, USA) with a frequency of 3 to 15 min during flood events and daily during non-flood events. Flow was computed from the shape of the river bed and the measured water level. Water quality was also monitored using an automatic water sampler (EcoTech Umwelt-Meßsysteme GmbH, Bonn, Germany) with 8 bottles, 2 L each. Sampling waters were for the same elements monitored in the erosion plots, with frequency varying from 3 min (during flash floods) to 15 h (during larger flood events). Further details can be found in Ramos et al. [21,22].

2.2.4. Enxoé Reservoir

The water quality in the reservoir was monitored at three locations (in the upper and middle reservoir and next to the dam wall) and two depths (near the surface and at the bottom of the reservoir) from September 2010 to March 2012. The reservoir was monitored for the vertical temperature profile, pH, potential redox, dissolved O_2 , EC, turbidity, SSC, organic matter, TP, SRP and NO_3^- . Composite samples from euphotic zone were used to identify the phytoplankton and quantify chlorophyll-a and specific biovolume (which is commonly calculated to assess the relative abundance, in terms of biomass or carbon, of co-occurring algae of various shapes and sizes). Sediment samples were also collected at the bottom of the reservoir for characterizing the vertical structure of sediment, the evolution of bottom sediment and the relation between Fe and P [19]. The state of the Enxoé reservoir was further assessed using measured data from Sistema Nacional de Informação de Recursos Hídricos (SNIRH) [35] for the period 2001–2011.

2.3. Modelling Approach

Four different models were used to assess sediment and nutrient dynamics in the Enxoé catchment and reservoir. The Soil Water Assessment Tool (SWAT) [36] is a semi-distributed, process-oriented model for simulating those processes at the catchment scale. The model divides the watershed into sub-basins and hydrological response units (HRU) that are homogeneous in terms of land use, soil, and slope. Model hydrology is based on the computation of the daily water balance, which accounts for crop evapotranspiration, infiltration, surface runoff, percolation, rainfall interception, groundwater and lateral flow and channel routing. Erosion and sediment yields are estimated for each HRU with the Modified Soil Loss Equation [37]. Nutrient dynamics includes inputs from agriculture, transport with runoff and groundwater, plant consumption and soil mineralization processes [36]. Brito et al. [23] applied this model to simulate sediment and nutrient long-term dynamics in the Enxoé catchment and respective loads to the reservoir. The reservoir inflows were calibrated and validated through

the computation of the reservoir water balance using rainfall and the reservoir volume, discharge, and evaporation data from January 2006 to August 2009. Nutrient dynamics was calibrated and validated using data collected at the sampling station located at the outlet of the catchment before the reservoir between September 2010 and August 2013 (Section 2.2.3). Soil erosion predictions were further qualitatively compared with erosion data measured in the field plots installed in two of the main land uses (olive trees and agro-forestry of holm oaks) between October 2009 and April 2013 (Section 2.2.1). After model calibration, SWAT was used to compute the water, sediment, and nutrient budgets for a 30-year period (1980–2010).

The MOHID-Land model [38] is an open-source, distributed, physically based model capable of simulating sediment and nutrient dynamics at the catchment scale. The surface runoff is computed with the full St. Venant equations and consider flooding, backwater movement and the drying process of the riparian zones. The surface runoff depends on exfiltration and infiltration processes. The saturated and vadose zones are computed simultaneously without an explicit interface. The porous media is defined using a 3D grid. The Richards equation is then used for computing flow in the porous media, while infiltration can be computed using Darcy's equation and surface pressure due to surface runoff water column or using empirical algorithms. A variable time-step is used to increase accuracy during rainfall or irrigation events (i.e., when soil moisture or surface water volumes changing rate is high). This feature makes the MOHID-Land model more suitable for the detailed analysis of flash floods in small watersheds as Enxoé, where concentration times can last only a couple of hours, than the SWAT model, which uses a daily time-step. Brito et al. [24] performed model calibration/validation by comparing model predictions of monthly inflows to the reservoir against those from the reservoir budget (2006–2009), as in SWAT. More detailed model evaluation was further carried out at the sampling location at the outlet of the catchment by comparing MOHID-Land predictions of the river water level with measured values collected between 2010 and 2011 (Section 2.2.3).

The CE-QUAL-W2 model [28] is a bidimensional, laterally averaged, dynamic model for simulating water quality at the reservoir scale. The Navier–Stokes equations are used for calculating the hydrodynamics component, namely the incompressible flow in the water body velocity field and turbulent diffusion coefficients. The water quality component is based on property sources and sinks, considering interactions between temperature, algae, nutrients, organic matter, dissolved O_2 and sediment [28]. Brito et al. [27] calibrated the model by adjusting input parameters until deviations between measured data and respective simulations of daily reservoir water levels and monthly concentrations of NO_3^- , SSC, orthophosphate, chlorophyll-a and dissolved O_2 were minimized. The model boundary conditions included daily river inputs of NO_3^- , NH_4^+ , organic matter, orthophosphate, SSC and O_2 computed with SWAT [23]. Measured values were obtained from the monitoring activities carried out between September 2010 and March 2012 (Section 2.2.4) or from SNIRH [35] for the period 2001–2011.

Finally, the PESERA model [26] is a physically based, frequency distributed, continuous prediction model for quantifying monthly and annual soil erosion rates at the plot and catchment scales. Rodrigues et al. [25] implemented this model for mapping soil erosion risks in the Enxoé catchment using local weather, soil, topography, and land use information, being then validated by comparing soil erosion risks with erosion rates measured in field erosion plots (Section 2.2.1).

3. Application of the DPSIR Framework to the Enxoé Catchment

The development of the DPSIR framework for the Enxoé catchment and reservoir summarized in Figure 2.

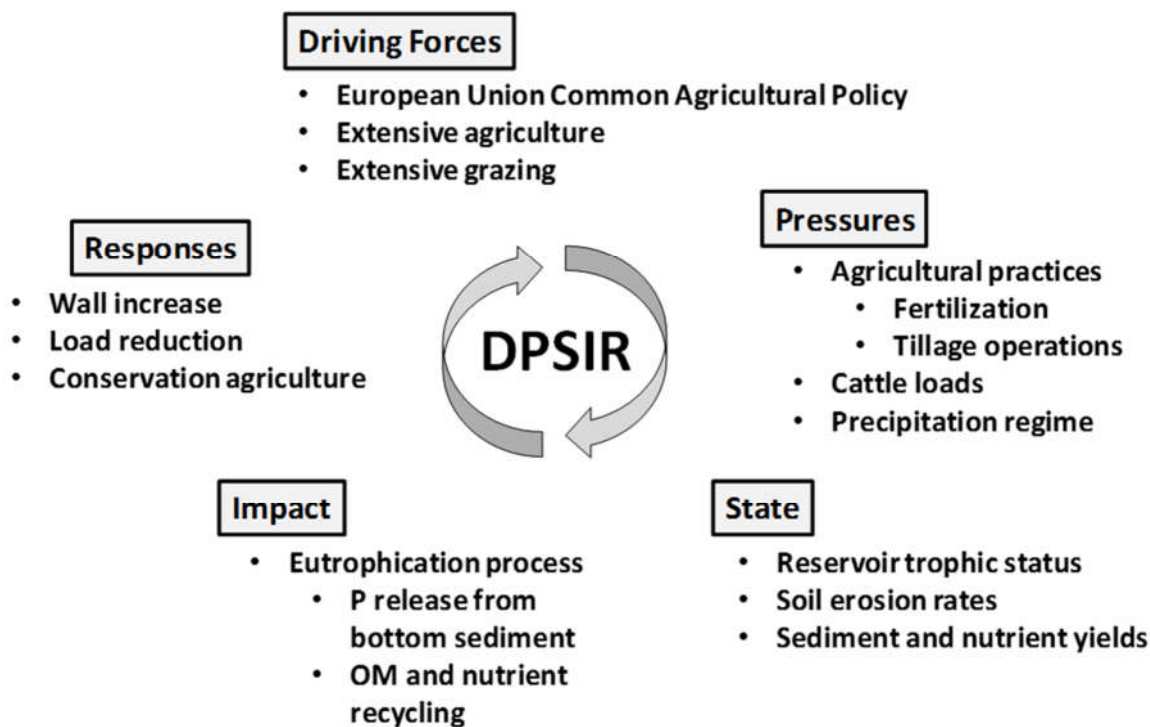


Figure 2. DPSIR conceptual scheme for the Enxoé catchment.

3.1. Driving Forces

Agriculture and extensive production of cattle were identified as the main driving forces in the Enxoé catchment (Figure 2). Agriculture activities in the region were economically supported by European Union subsidies, namely by the single payment scheme for farmers under the common agricultural policy. Direct aids were also given for maintaining farming in severely disadvantage European regions such as Enxoé, partially compensating farmers for the additional costs and income losses of farming in unfavorable areas (e.g., mountainous areas, climate conditions, poor soils); for environmental protection and maintenance of the agro-forestry of holm oaks system (locally known as “montado”) and olive groves heritage; and for maintaining suckler cows, sheep and goats. Complying with these policies conditioned agricultural practices and, thus pressures in the catchment. Similar analyses have been conducted in other Mediterranean catchments, highlighting the role of agriculture and European funding as the main driving forces for water quality problems in those regions [31,39–41].

3.2. Pressures

Agricultural practices (tillage operations and fertilization inputs), cattle load and the precipitation regime were identified as the main pressures in the region (Figure 2), in line with the existing literature [2,31,39].

Olive orchards were divided between traditional (<100 trees ha⁻¹) and more intensive (300–500 trees ha⁻¹) systems. Tillage operations were minimal and usually only carried out for weed control in areas with traditional olive orchards, while irrigation was applied in more intensive orchards during summer (200 mm·year⁻¹). N inputs ranged between 24 and 60 kg ha⁻¹, with the lower values being applied in the traditional orchards. P inputs were small (15 kg ha⁻¹), being applied only in the intensive orchards. Fertilization was limited to the spring season. Sheep grazing reached 0.1 livestock units (LSU).

The “montado” system is an open savannah-like landscape predominant in the south of the Iberian Peninsula. It results from an extensively managed agro-silvo-pastoral system [42], where holm oak (*Quercus ilex rotundifolia* L.) and cork (*Quercus suber* L.) trees present high levels of spatial variability

in terms of density combined with fallow land or pastures, that can be natural, improved, or cultivated. The system is further considered of High Natural Value, providing various ecosystem services that are perceived by farmers, technicians, stakeholders, and society in general as being important for human welfare. As such, tillage operations were minimal and carried out for sowing annual winter crops in areas with less than 30 trees ha⁻¹ or for preventing forest fires. Fertilization was only applied in areas with annual winter crops (usually oats). Grazing (cows, sheep, goats, and swine) was limited to 0.4 LSU, increasing to 0.6 LSU for 3 months during the holm oaks fructification period.

Annual winter (wheat, triticale, barley, and oats) and summer (sunflower) crops were mainly sowed during autumn and spring, respectively, usually using heavy tillage techniques (moldboard plowing and harrowing) for preparing the seedbed. Most crop rotations included fallow. N and P inputs varied between 20–90 and 18–60 kg ha⁻¹, respectively, applied during the autumn and spring seasons. Grazing (cows and sheep) reached 0.6 LSU.

Fertilization inputs were estimated to globally average 25.40 kg N ha⁻¹ year⁻¹ and 11.68 kg P ha⁻¹ year⁻¹ in the catchment area. However, it is important to understand that these estimates were obtained by inquiring farmers in the region and thus should be merely indicative. Based on the LSU, animal excretions were also estimated to reach 25.69 kg N ha⁻¹ year⁻¹ and 3.04 kg P ha⁻¹ year⁻¹. Hence, nutrient inputs in the catchment were considered relatively low when compared with other more intensive agricultural areas [43].

The precipitation region was also identified as one of the main pressures influencing the Enxoé catchment, conditioning the hydrological regime and nutrient dynamics in the region. Total precipitation summed 695, 270 and 570 mm during the 2010/2011, 2011/2012 and 2012/2013 hydrological years, respectively. Annual river discharge yielded 28.73, 1.27 and 10.14 hm³ for the same period (Figure 3). The flow regime in the Enxoé River varied along the hydrological year and was characterized: (i) by the existence of no flow or ephemeral conditions from June to September; (ii) the generation of flow peaks from September to October (i.e., the beginning of an hydrological year), being these quickly reduced as the soil was still dry and groundwater flow was diminished; (iii) soil profile saturation as a result of heavy rain occurring from October to December, enhancing subsurface flow and producing flood events with multiple discharge peaks; and (iv) longer groundwater flows as the soil remained saturated from December to April, but which still tended to fall quickly especially during months with less rain (January/February).

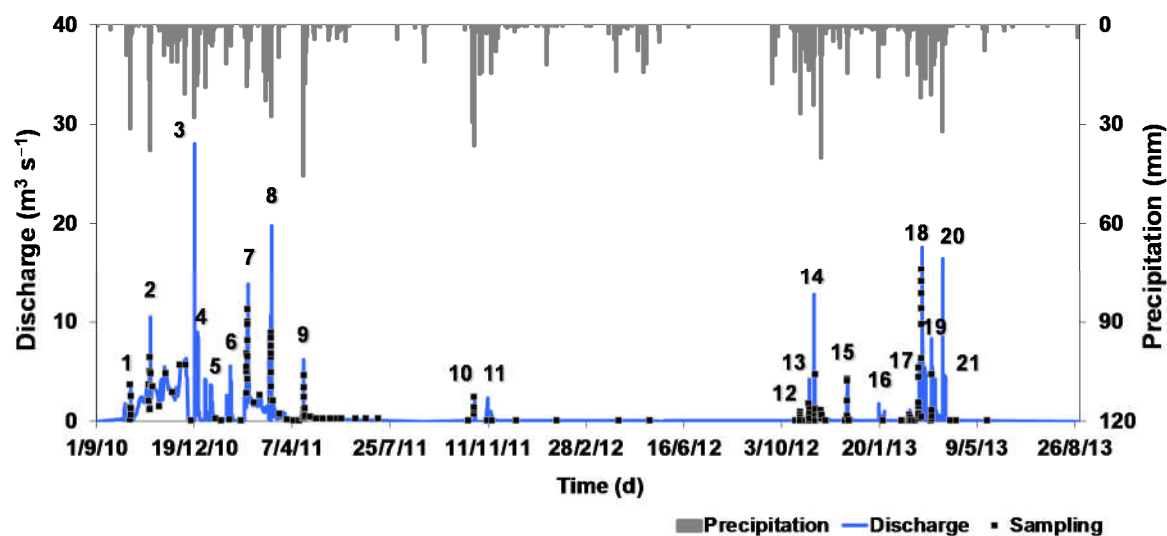


Figure 3. Precipitation and discharge at the monitoring outlet between September 2010 and August 2013.

Hence, while flow in the Enxoé River was mostly influenced by rainfall events, the effect of groundwater table was not significant. Twenty-one flash foods occurred between September 2010 and

August 2013, taking place during autumn (10), winter (8) and spring (3) (Figure 3). These flash flood resulted mostly from high-intensity, convective or convective-enhanced storms, which were already associated with high sediment and nutrient yields in different catchments in the world [44–48].

3.3. State

The state evolution of the Enxoé catchment was characterized based on sediment and nutrient loads to the reservoir as well as in terms of key parameters contributing to water quality (Figure 2).

3.3.1. Field Scale

Soil erosion in plots 1, 2 and 3 averaged 126, 189 and 20 kg ha^{−1} year^{−1}, respectively and ranged from 1.3 to 405 kg ha^{−1} year^{−1} during the three monitored years (Table 1). The lowest values were obtained during the dry 2011/2012 hydrological year. The highest value was observed in Plot 2 at the beginning of the monitored period (2009/2010) when trees were only 8 years old. Soil erosion then progressively decreased during the following years as tree canopy increased providing for better protection of the soil surface against raindrop impact and particle detachment. Soil erosion rates at all three monitored plots were relatively low and perfectly within the threshold limits (1000–2000 kg ha^{−1} year^{−1}) suggested by Huber et al. [49] as tolerable for southern Europe. Table 1 also presents annual TP, NO₃[−], POC and DOC yields monitored in the three erosion plots. Despite concentrations were relatively high (Figure 4), annual yields were only residual due to the small number of events producing runoff.

Field plot measurements of soil erosion were limited to a very short period which implies that they were not necessarily representative of long-term erosion rates [50]. However, one advantage of the design used was that erosion plots were not closed and thus there was no exhaustion of available material for soil detachment which can occur with the creation of an armor layer on the soil surface and the lack of input of transported material from outside. The draining area of each plot continued to be influenced by local agricultural practices and grazing, with only the collecting system being protected with a barbed wire fence.

Erosion plots results corresponded to Rodrigues et al. [25] predictions that approximately 65% of the catchment area presented a potential soil loss rate lower than 0.5 t ha^{−1} year^{−1} (Figure 5). This low erosion risk corresponded mostly to areas with olive orchards and “montado”, which were subjected to extensive farming and grazing, providing an important protection against soil erosion since the soil was covered with vegetation for most part of the year. The areas with higher erosion risk (over 50 t ha^{−1} year^{−1} of estimated soil loss) corresponded to approximately 19% of the total area and were mainly located in the northwest and southeast of the basin, where a more intensive agriculture prevailed (Figure 1).

Table 1. Soil and nutrient yields in the Enxoé catchment.

Element	Erosion Plots			Enxoé River (kg ha ⁻¹)
	Plot 1 (kg ha ⁻¹)	Plot 2 (kg ha ⁻¹)	Plot 3 (kg ha ⁻¹)	
Sediment:				
2009/2010	85.5	405.0	-	-
2010/2011	96.3	255.4	-	480.2
2011/2012	79.7	58.3	1.3	12.5
2012/2013	242.1	36.4	38.8	369.4
Total	503.6	755.1	40.1	862.1
Annual yield	125.9	188.8	20.1	287.4
TP:				
2009/2010	0.04	0.19	-	-
2010/2011	0.07	0.16	-	0.96
2011/2012	0.08	0.02	0.00	0.04
2012/2013	0.06	0.03	0.11	0.84
Total	0.26	0.40	0.12	1.84
Annual yield	0.07	0.10	0.01	0.61
NO₃⁻:				
2009/2010	0.13	0.26	-	-
2010/2011	0.35	0.14	-	45.53
2011/2012	0.15	0.13	0.01	4.38
2012/2013	0.50	0.09	1.13	15.07
Total	1.14	0.61	1.14	64.98
Annual yield	0.29	0.15	0.57	21.66
POC:				
2009/2010	1.98	5.86	-	-
2010/2011	0.46	5.03	-	215.0
2011/2012	0.53	15.43	0.08	6.0
2012/2013	2.46	0.72	1.52	166.0
Total	5.42	24.04	1.60	387.0
Annual yield	1.36	6.76	0.80	129.0
DOC:				
2009/2010	0.95	1.16	-	-
2010/2011	0.96	0.65	-	147.0
2011/2012	0.07	0.20	0.06	3.0
2012/2013	0.91	0.19	1.56	68.0
Total	2.89	2.20	1.62	218.0
Annual yield	0.72	0.55	0.81	72.6

Annual precipitation in 2009/2010, 2010/2011, 2011/2012 and 2012/2013 amounted 494, 695, 270 and 570 mm, respectively.

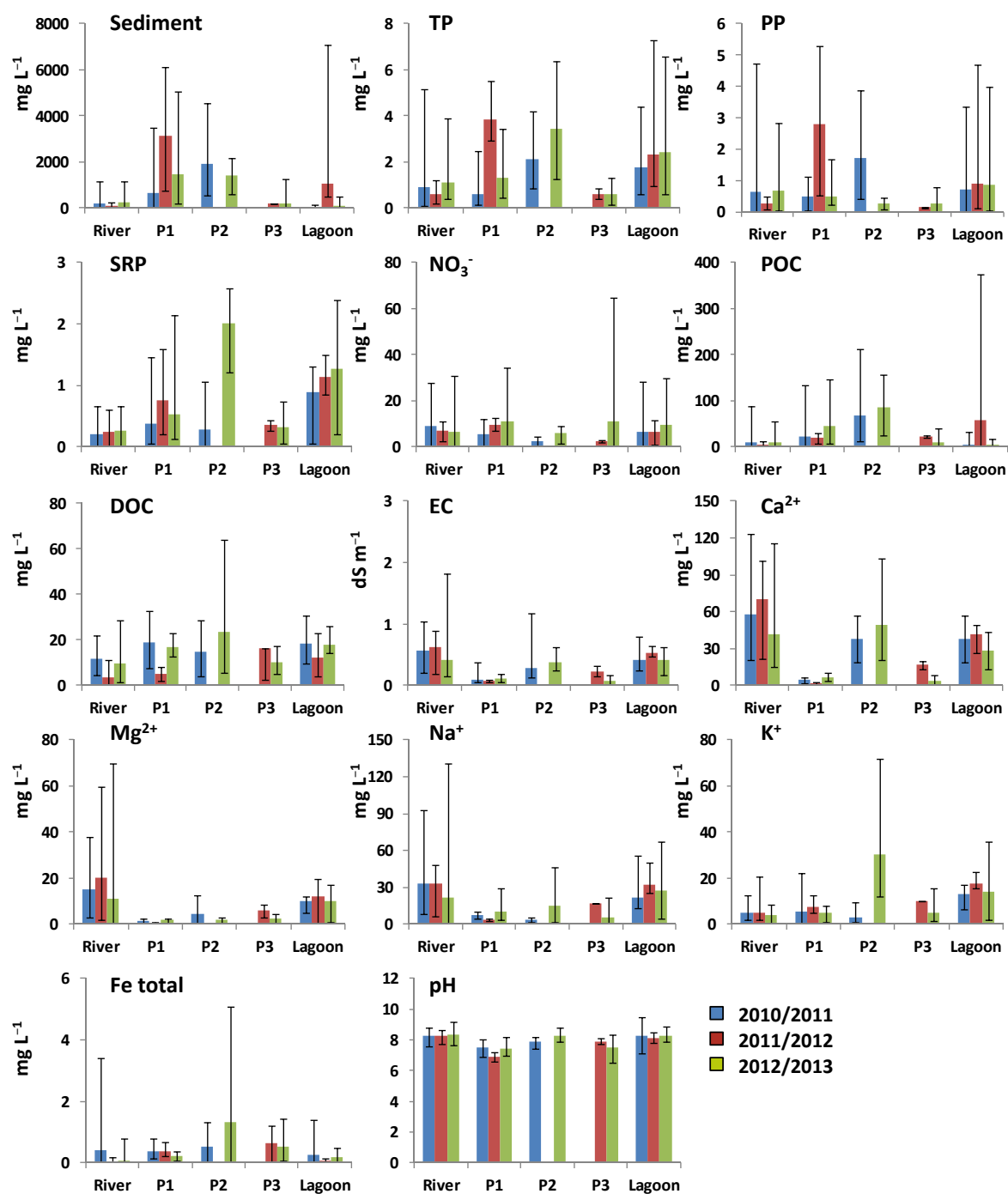


Figure 4. Sediment and nutrient concentrations in the Enxoé River, erosion plots (P1, P2 and P3) and lagoon (TP, total phosphorus; PP, particulate phosphorus; SRP, soluble reactive phosphorus; POC, particulate organic carbon; DOC, dissolved organic carbon; EC, electrical conductivity). Vertical bars refer to maximum and minimum values monitored.

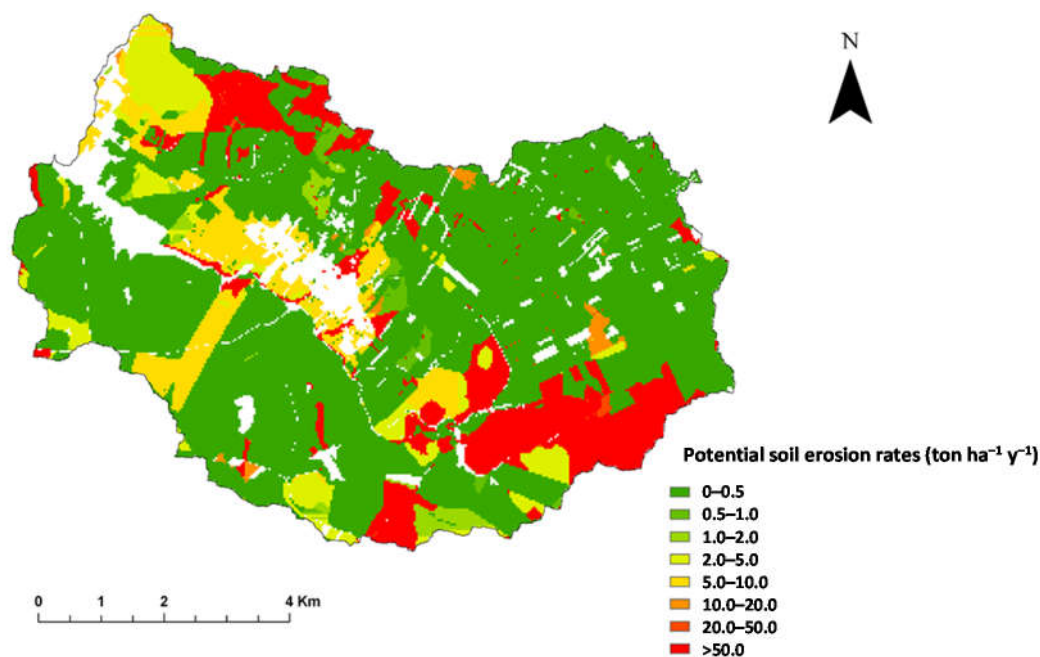


Figure 5. Soil erosion risks in the Enxoé catchment using the PESERA model.

3.3.2. Catchment Scale

Field plot soil erosion measurements cannot be linearly upscaled to the catchment due to the specificity of the processes that take place at a specific scale but also at the connection between scales [51]. As explained by Cammeraat [52], Mediterranean areas are characterized by a mosaic of run-on and runoff patches which determine the hydrological and erosional response at the hillslope level. The size and distance to the runoff generating area separated with areas with high water adsorption capacity explains why it is impossible to extrapolate plot scale runoff to the catchment scale and why the location of measurements strongly influences the results [51]. For that, the Enxoé River was also monitored at the outlet of the catchment to have a better assessment of sediment and nutrient loads to the reservoir.

Figure 4 presents the large variability observed in the concentrations of the different elements monitored in the Enxoé River. Mean concentrations of the particulate elements (SSC, TP, PP and POC) were generally lower in the river than in the erosion plots and lagoon. Boix-Fayos et al. [51] attributed this to the effect of sediment sinks, which often becomes dominant over sediment sources, resulting in a gradual decline in sediment yield. Osterkamp and Toy [53] defined this as a change in the system from erosion-limited to transport-limited conditions. The larger the area, the greater the likelihood of sediment deposition on the way. As such, sediment yields at the basin outlet may be lower than erosion rates measured on field erosion plots. In Enxoé, maximum values were always observed during flash flood, namely during autumn and spring, being responsible for 59–92% of the annual transport. Minimum values were mostly observed during non-flood events.

A flushing behavior, i.e., the increase of solute concentration with the arrival of the discharge peaks, was always monitored for the particulate elements (SSC, TP, PP and POC) (Table 2). The transport of these elements was thus associated with surface runoff and soil erosion. Tillage operations and grazing the river bed were the main activities associated with particle availability and soil erosion [21]. On one hand, tillage operations carried out in fields with annual winter crops at the same time heavy rains were registered (autumn and early spring) ended up enhancing soil erosion by removing the soil cover surface provided by crop residues or growing plants, reducing the capacity to absorb the energy of raindrops and to reduce the erosive energy of runoff and promoting also aggregate destruction and particle detachment. On the other hand, grazing the river bed during drier seasons also often led to bank destruction and trampling, affecting bank stability, stabilization, and accretion and thus flow

erosion. Bull [54] refers to the mechanisms on how vegetation contributes to prevent bank erosion, namely, by retarding the near-bank flow and damping turbulence, by resisting tension and increasing cohesion and by reducing the impact of moisture and loosening processes, which are a precursor to the removal of materials. Therefore, grazing the river bed can enhance bank erosion, with the eroded bank materials adding to the deposited sediment stock in the river bed, increasing the quantity of available particles that can be easily transported by storm events [55]. Bull [54] estimated that the contribution of bank eroded materials to river sediment systems may vary between less than 5 to over 80%. In Enxoé, such estimate was not possible to reach. However, the source of the eroded materials was identified for each storm event based on the interpretation of hysteresis in the concentration-discharge relationships following Butturini et al. [56] (Table 2). The analysis of the shape, rotational patterns, and trends of the hysteretic loops of each particle element during flash floods allowed to identify the dominance of close-by sources (particularly river beds) during most of autumn events, but also during spring. During winter and spring, agricultural fields were identified as the most likely sources of the eroded particulate materials [21,22].

In contrast, mean concentrations of the soluble elements (SRP, DOC, EC, Ca^{2+} , Mg^{2+} , K^{+} and Na^{+}) were generally higher in the Enxoé River than in the erosion plots and lagoon (Figure 4), mostly because the main transport mechanism for these elements was not related to soil erosion. The transport of the soluble elements was mainly associated with subsurface flow and essentially resulted from soil weathering processes, the mineralization of the soil humus fraction and the mineralization of crop residues and other organic wastes. These elements typically showed a dilution behavior, i.e., the decrease of solute concentration with the arrival of the discharge peaks (Table 2). Only NO_3^{-} presented a distinct behavior when compared with other soluble elements due to fertilization. NO_3^{-} yields were regularly observed during autumn and spring (rain season), when crop fertilization was expectably carried out. Thus, this element registered a flushing behavior during autumn as a result of successive rainfall events observed during that period, saturated soils and soil physical characteristics that favored leaching as shown by the dominant anticlockwise hysteresis loops monitored during discharge peaks (Table 2) (i.e., concentration peaks arriving only at the monitoring station after discharge peaks); an indicator of NO_3^{-} transport from distant source areas [56]. During winter and spring, the flushing mechanism switched to a dilution behavior (Table 2) with the arrival of water from non-fertilized areas (permanent pastures, agro-forestry of holm oaks).

Ramos et al. [21,22] estimated the annual sediment and nutrient yields based on the monitored data (Table 2). Average sediment and NO_3^{-} yields amounted 287.4 and 21.66 kg ha⁻¹ year⁻¹, respectively and were considered relatively small when compared with reports from other Mediterranean catchments [46,57,58]. Annual TP, POC and DOC yields reached 0.61, 129.0 and 72.6 kg ha⁻¹ year⁻¹, being considered relatively high but also comparable to other Mediterranean catchments [58–60].

SWAT long-term model predictions confirmed the previous yield estimates determined from field data. The 30-year simulation period (1980–2010) revealed that approximately 80–85% of the annual rainfall was evapotranspired and that the remaining 15–20% was delivered to the river [23]. Average annual sediment yield was also relatively low (450 kg ha⁻¹ year⁻¹) and comparable to the first and third monitored years when no drought occurred (Table 1). However, SWAT simulations showed some sub-basins producing values up to 1000–2000 kg ha⁻¹ year⁻¹, thus reaching the numbers of Walling and Webb [57] for some catchments in the Iberian Peninsula. NO_3^{-} loads were within the same order of magnitude (12 kg ha⁻¹ year⁻¹) of field measurements, while TP yields were found to be smaller (0.3 kg ha⁻¹ year⁻¹) than those measured in the Enxoé River (Table 1).

Brito et al. [24] produced similar estimates for NO_3^{-} yields using the MOHID-Land model, but the effective annual P transport to the reservoir was found to be up to three times the average annual P load estimated by SWAT. This was explained by the capacity of the MOHID-Land model in using a variable time-step (of the order of seconds or less) to describe flash flood formation and propagation, which SWAT could not. As such, despite the both models considered the same P loads arriving to the river

network, SWAT then deposited a significant part on the riverbed, while MOHID-Land showed that the deposited material would later be resuspended during flash floods and transported to the reservoir.

Table 2. Sediment and nutrients sources and main transport mechanisms in the Enxoé catchment.

Element ^a	Autumn			Winter			Spring		
	Source ^b	Transfer ^c	Pattern ^d	Source ^b	Transfer ^c	Pattern ^d	Source ^b	Transfer ^c	Pattern ^d
Particulate elements —SSC, TP, PP and POC	RB	R	F/AC	AF	R	F/M	RB/AF	R	F/M
Soluble elements —SRP	RB/AF	R/LF	D/M	RB	R	F/AC	RB	R	F/AC
—NO ₃ [−]	AF	LF	F/AC	AF	LF	D/M	AF	LF	D/AC
—DOC	AF	LF	D/AC	AF	LF	D/AC	AF	LF	D/AC
—EC	—	LF	D	—	LF	D	—	LF	D
—Na ⁺ , Ca ²⁺ , Mg ²⁺ , K ⁺	—	LF	D	—	LF	D	—	LF	D
—Total Fe	—	LF	D	—	LF	D	—	LF	F

Notes: ^a SSC, suspended sediment concentration; TP, total phosphorus; PP, particulate phosphorus; SRP, soluble reactive phosphorus; NO₃[−], nitrate; POC, particulate organic carbon; DOC, dissolved organic carbon; EC, electrical conductivity. ^b RB, river bank; AF, agricultural field. ^c R, runoff; LF, lateral flow. ^d F, flushing; D, dilution; M, mixed; C, clockwise; AC, anticlockwise

3.3.3. Reservoir Scale

Reservoir monitoring was carried out in three sites (lotic zone at the beginning of the reservoir, transition zone in the center, lacustrine area near the dam wall) between September 2010 and March 2012. Water temperature data from the reservoir dam measured profiles (17 m at deep full storage) showed a clear thermal stratification during the summer months (June to August), with differences between surface and bottom temperatures reaching 10 °C. The thermocline was also observed at 4–8 m depth. During winter months, stratification disappeared due to stronger winds and lower surface air temperatures. Homogeneous and colder temperature profiles were then observed [27]. The dissolved O₂ profiles taken near the Enxoé dam showed similar seasonal patterns as those for temperature. Stratification was observed during summer months (June to August), with the maximum difference between surface and bottom concentrations totalizing 5–10 mg L^{−1}. O₂ changes were very pronounced in the thermocline at 4 m due to the existence of bottom sink processes (mineralization, nitrification), which occurred as the capacity to oxygenate was reduced with depth promoting anoxic conditions in the sediment and water column that originated the liberation of adsorbed P. In aerobic conditions, Fe³⁺ bounds with P and forms an insoluble complex locking up P in a form that algae cannot access. However, in anaerobic conditions, Fe³⁺ is chemically reduced to Fe²⁺, releasing P and making it available to algae [61]. Hence, vertical density stratification of the water body (common in summer) reduced vertical diffusion of O₂ and promoted anoxic conditions at the bottom of the Enxoé reservoir. In the winter months, stratification disappeared. Homogeneous profiles were then observed, showing higher dissolved O₂ concentrations [27].

Surface SSC showed base and peak values of 10 and 60–70 mg L^{−1}, respectively, between 2001 and 2011 [35]. Surface NO₃[−] concentrations measured also during the same period were very low, ranging from 1 to 0.5 mg L^{−1} at the surface [35], while data from water profiles showed relatively higher concentrations (up to 8 mg L^{−1}) [19]. Surface SRP concentrations ranged from 0.02 to 0.1 mg L^{−1} at the surface (2001–2011), while TP averaged 0.1 mg L^{−1} at the surface and higher than 0.035 mg L^{−1} along the water profile.

Measured surface chlorophyll-a concentrations presented a geometric average of 33 µg L^{−1} for the period 2001–2011, varying between minimum values on the order of units of µg L^{−1} and maximum values above 200 µg L^{−1} [35]. This geometric average corresponded to eutrophic, being higher than the 10 µg L^{−1} defined as the national threshold limit for eutrophication. Morais et al. [19] confirmed the high productivity of the phytoplankton community (in 87.5% of the measurements above the limit for the good ecological potential status). In terms of taxonomic composition, cyanobacteria were dominant in the summer season, in some situations with 100% of relative abundance and with densities showing the existence of blooms formed by potentially toxic taxa. This gradient evidenced

the entry of allochthonous materials to the system (mainly evidenced by greater turbidity), reinforcing the need to apply measures and to define effective policies for management.

3.4. Impacts

The sediment and nutrient loads to the reservoir described impacts of the catchment to the eutrophication of the Enxoé reservoir (Figure 2). After the calibration of the CE-QUAL-W2 model, the measured field data (surface and profiles) was simulated with success. Brito et al. [27] computed the N and P budgets of the reservoir to understand the main processes responsible for sustaining the high trophic level observed. The estimated average N and P annual fluxes in each component (river inflow, reservoir outflow, algal assimilation/respiration, denitrification, mineralization, sediment release under anoxic conditions, organic matter decay and zooplankton respiration) were accounted for the period 2001–2011.

For N, 17 ton year^{−1} (60% of the input) were removed from the reservoir with outflow; a high level of N recycling existed due to algal N assimilation/death and consequent organic matter decay, including denitrification under anoxic conditions (most part of the summer). For P, 0.83 ton year^{−1} (140% of the input) were removed with outflow, while 0.6 ton year^{−1} (100% of the input) were generated from sediment bottom release; the internal P recycling processes (algal assimilation, mineralization, or organic matter decay) removed 55% of the P input (0.33 ton year^{−1}).

The Enxoé reservoir behaved as a nutrient recycler between algal cycles, with reduced dependency on watershed inputs because of cyanobacteria dominance, which were able to assimilate atmospheric N₂ and were sustained by internal sediment P (of the same order as the catchment input). Similarly, Søndergaard et al. [62] demonstrated the importance of internal P loading to the high trophic level registered in Lake Arresø (Denmark). Their study area presented a relatively high sediment P release rate during resuspension because of the type of sediment and low Fe-P ratio. Those authors inferred that the internal P release contributing to a reservoir's high trophic level could last for several decades, even when external loading was reduced. Likewise, Lee and Oh [9] referred that the sediment release fluxes were considerable compared to loads from the catchment, highlighting the need for reducing the internal pollutant loads in four reservoirs in South Korea.

3.5. Response

The response of the Enxoé reservoir to different management scenarios has been assessed through modelling over the years. For example, ARH Alentejo [18] considered different river load reduction scenarios using the CE-QUAL-W2 model. Chlorophyll-a concentration responded to scenarios of 40 to 90% load decrease, with values ranging from 26.9 to 42.6 µg L^{−1} depending on the scenario. These still corresponded to eutrophic levels though. As such, those authors recognized the importance of flash floods for sediment and nutrient dynamics, but also the role of P remobilization in fueling algae blooms under anoxic conditions. They then advanced with some mitigation measures, which included the removal of the deposited sediment at the bottom of the reservoir and the construction of ditches to trap sediment upstream.

On the other hand, Ramos et al. [21] suggested management practices for reducing soil erosion risks in arable lands of the catchment. These included the promotion of reduced tillage techniques to effectively reduce sediment losses, maintaining crop residue at the soil surface and minimizing soil particle detachment and movement during storms. They further recommended the protection of river banks and riparian vegetation, contributing to bank stability and cohesion.

Finally, Brito et al. [27] considered five management scenarios, which included the reduction of P load in the Enxoé River by 50%, the removal of sediment P load and the increase of the dam wall up to 2 m (average depth of the reservoir would then be 7 m instead of the current 5 m). The scenario testing the dependence on internal load (no river load) showed reductions of 13% for mean and maximum chlorophyll-a concentrations during the entire simulation period (2001–2010) when compared to current conditions, these being hardly noticeable over the years since internal P loads would still be

able to fuel algal blooms for months. The scenario with 50% P load reduction (from river input and bottom sediment) led to a reduction of chlorophyll-a mean and maximum concentrations between 47 and 52% when compared to current conditions. Only the scenario with a 50% P reduction from river input and complete removal of the internal P load resulted in a 75–78% reduction in the mean and maximum chlorophyll-a concentrations when compared to current conditions. In this case, mean chlorophyll-a concentration values yielded 12–14 $\mu\text{g L}^{-1}$ (geometric averages of 7–8 $\mu\text{g L}^{-1}$), being difficult to sustain it as safe though. Thus, Brito et al. [27] concluded that decreasing loads to these levels would require: (i) reducing the suspended material inflow to the reservoir especially during flash flood, which would mean placing retention barriers upstream to retain sediment, preserving riparian vegetation and promoting conservation tillage practices in the catchment, in line with ARH Alentejo [18] and Ramos et al. [21]; and (ii) removing anoxia from the reservoir bottom through O_2 aeration at the reservoir bottom. This later solution was also proposed by Lee and Oh [9] for South Korean reservoirs, with these requiring aeration in the bottom when anoxic conditions were present. These authors further suggested that for reservoirs subjected to livestock pollution sources, priority should be given to sediment management, namely by seasonally supplying O_2 to the bottom of the reservoirs to control the release rate of contaminants from sediment.

Finally, following INAG [17], who reported that most of the reservoirs in Portugal with mean depths of less than 10 m presented eutrophic conditions even with low urban or diffuse loads, Brito et al. [27] demonstrated that with a 2-m wall increase (no load reductions), chlorophyll-a concentrations in the Enxoé reservoir would reduce 82–91% (mean values of 5–10 $\mu\text{g L}^{-1}$ and geometric mean of 3–6 $\mu\text{g L}^{-1}$) when compared to current conditions. Therefore, while reducing the P load by 75% (externally from catchment sources and internally from the bottom sediment source) could reduce the reservoir trophic level to values close to the eutrophication limit, only by limiting the P internal load ability to reach the photic zone in parts of the reservoir would lead to a sustainable mesotrophic state level. Nonetheless, Jarvie et al. [63] adverted for the fact that P-based mitigation measures may not be the most effective strategies for combating freshwater eutrophication. These would require the control of additional nutrients. Those authors justified that since ecosystem recovery does not always follow the trajectories of stressor-response models because of the long-term lags associated with the legacy of P from past land use management. Also, P reductions fail to reach the challenging limitation thresholds for algal growth. Finally, the decoupling of algal biomass response to P concentrations result from multiple physical-chemical and biological factors, not only P.

4. Conclusions

This study presented an integrated analysis of the eutrophication process in the Enxoé River and reservoir (southern Portugal), with the DPSIR framework providing a common context for research carried out in the region over the last few years. The drivers provided the identification of the major causes affecting water quality in the Enxoé reservoir. The pressures highlighted the way these drivers were expressed. The state provided the current environmental status of the Enxoé catchment and reservoir. The impacts identified the causative effects leading to the eutrophication of the reservoir. The response emphasized the results by considering different pressure change scenarios.

Although agriculture and grazing were the main driving forces in the catchment, annual sediment and nutrient loads were found to be relatively small to medium and comparable to those reported for similar Mediterranean catchments. These values were already expected for an extensive agricultural area with gentle slopes (low erosion) and reduced human presence. However, the precipitation regime and the formation of flash floods proved to be fundamental for sediment and nutrient dynamics, with these events being in some cases able to transport up to three times the average annual load.

While a relation was found between flash floods and chlorophyll-a blooms in the Enxoé reservoir, the main eutrophication process was verified to be the release of P from bottom sediment under anoxic conditions and the process of internal recycling that would be able to sustain high algal concentrations for months (algal and organic matter decay and nutrient assimilation and decay). This was confirmed

by the management scenarios tested using the CE-QUAL-W2 model, showing the importance of reducing the P load by 75% (from the catchment and internal sources) for reaching a mesotrophic state level in the reservoir. However, this trophic level would only be sustainable by limiting the P internal load ability to reach the photic zone.

Author Contributions: T.B.R. and H.D. wrote the paper; D.B. run model simulations; M.A.B. performed the laboratory analysis; J.C.M., M.L.F. and F.P. conducted the field catchment work; M.M. carried out reservoir monitoring; M.C.G. and R.N. revised a first draft version of this paper.

Funding: This study was funded by the EUTROPHOS project (PTDC/AGR-AAM/098100/2008) of the Foundation for Science and Technology (FCT) and the AGUAMOD project (<http://www.aguamod-sudoe.eu/pt/>) of the INTERREG SUDOE program. MARETEC acknowledges the national funds from FCT (Project UID/EEA/50009/2013). T. B. Ramos was supported by the FCT grant SFRH/BPD/110655/2015.

Conflicts of Interest: The authors declare no conflict of interest.

References

1. Kronvang, B.; Vagstad, N.; Behrendt, H.; Bøgestrand, J.; Larsen, S.E. Phosphorus losses at the catchment scale within Europe: An overview. *Soil Use Manage.* **2007**, *23*, 104–116. [[CrossRef](#)]
2. Song, X.; Frostell, B. The DPSIR framework and a pressure-oriented water quality monitoring approach to ecological river restoration. *Water* **2012**, *4*, 670–682. [[CrossRef](#)]
3. Halliday, S.J.; Skeffington, R.A.; Bowes, M.J.; Gozzard, E.; Newman, J.R.; Loewenthal, M.; Palmer-Felgate, E.J.; Jarvie, H.P.; Wade, A.J. The water quality of the River Enborne, UK: Observations from high-frequency monitoring in a rural, lowland river system. *Water* **2012**, *6*, 150–180. [[CrossRef](#)]
4. Honti, M. Controlling river eutrophication under conflicts of interest—A GIS modeling approach. *Water* **2015**, *7*, 5078–5090. [[CrossRef](#)]
5. Pinardi, M.; Fenocchi, A.; Giardino, C.; Sibilla, S.; Bartoli, M.; Bresciani, M. Assessing potential algal blooms in a shallow fluvial lake by combining hydrodynamics modelling and remote-sensed images. *Water* **2015**, *7*, 1921–1942. [[CrossRef](#)]
6. Rolighed, J.; Jeppesen, E.; Søndergaard, M.; Bjerring, R.; Janse, J.H.; Mooij, W.M.; Trolle, D. Climate change will make recovery from eutrophication more difficult in shallow Danish Lake Søbygaard. *Water* **2016**, *8*, 459. [[CrossRef](#)]
7. Zhang, W.H.; Xu, Q.J.; Wang, X.X.; Hu, X.Z.; Wang, C.; Pang, Y.; Hu, Y.B.; Zhao, Y.; Zhao, X. Spatiotemporal distribution in Lake Tai as affected by wind. *Water* **2017**, *9*, 200. [[CrossRef](#)]
8. Beklioğlu, M.; Bucak, T.; Coppens, J.; Bezirci, G.; Tavşanoğlu, Ü.N.; Çakıroğlu, A.I.; Levi, E.E.; Erdoğan, S.; Filiz, N.; Özkan, K.; et al. Restoration of eutrophic lakes with fluctuating water levels: A 20-year monitoring study of two inter-connected lakes. *Water* **2017**, *9*, 127. [[CrossRef](#)]
9. Lee, J.-K.; Oh, J.-M. A study on the characteristics of organic matter and nutrients released from sediments into agricultural reservoirs. *Water* **2018**, *10*, 980. [[CrossRef](#)]
10. Lee, R.M.; Biggs, T.W.; Fang, X. Thermal and hydrodynamics changes under a warmer climate in a variable stratified hypereutrophic reservoir. *Water* **2018**, *10*, 1284. [[CrossRef](#)]
11. Moreira, G.A.L.; Hinegk, L.; Salvatore, A.; Zolezzi, G.; Hölder, F.; Domecq, R.A.M.; Bocci, M.; Carrer, S.; Nat, L.D.; Escribá, J.; et al. Eutrophication, research and management history of the shallow Ypacaraí Lake (Paraguay). *Sustainability* **2018**, *10*, 2426. [[CrossRef](#)]
12. Rollwagen-Bollens, G.; Lee, T.; Rose, V.; Bollens, S.M. Beyond eutrophication: Vancouver Lake, WA, USA as a model system for assessing multiple, interacting biotic and abiotic drivers of harmful cyanobacterial blooms. *Water* **2018**, *10*, 757. [[CrossRef](#)]
13. Yu, C.; Li, C.; Wang, T.; Zhang, M.; Xu, J. Combined effects of experimental warming and eutrophication on phytoplankton dynamics and nitrogen uptake. *Water* **2018**, *10*, 1057. [[CrossRef](#)]
14. Vinçon-Leite, B.; Casenave, C. Modelling eutrophication in lake ecosystems: A review. *Sci. Total Environ.* **2019**, *651*, 2985–3001. [[CrossRef](#)]
15. Kawara, O.; Yura, E.; Fujii, S.; Matsumoto, T. A study on the role of hydraulic retention time in eutrophication of the Asahi River Dam Reservoir. *Water Sci. Tech.* **1998**, *37*, 245–252. [[CrossRef](#)]
16. Soares, M.C.S.; Marinho, M.M.; Azevedo, S.M.O.F.; Branco, C.W.C.; Huszar, V.L.M. Eutrophication and retention time affecting spatial heterogeneity in a tropical reservoir. *Limnologica* **2012**, *47*, 197–203. [[CrossRef](#)]

17. Instituto Nacional da Água (INAG). *Management of the Trophic Status in Portuguese Reservoirs. Report on Classification and Trophic State Reduction in the Scope of WWTP Directive*; Instituto da Água: Lisbon, Portugal, 2009; Available online: <https://www.apambiente.pt/?ref=16&subref=7&sub2ref=9&sub3ref=834> (accessed on 20 May 2018).
18. ARH Alentejo. *Planos de Gestão das Bacias Hidrográficas Integradas nas Regiões Hidrográficas 6 e 7. Região hidrográfica 7*; MAMAOT: Lisboa, Portugal, 2012; Available online: https://www.google.com/url?sa=t&rct=j&q=&esrc=s&source=web&cd=2&ved=2ahUKewjn2Y-_zLneAhVYQd4KHc31Du4QFjABegQIABAC&url=https%3A%2F%2Fsniambgeoviewer.apambiente.pt%2FGeodocs%2Fgeoportaldocs%2FPlanos%2FPGRH6%2FRelSintese%255CRS_RH6_RH7_VF.pdf&usg=AOvVaw325yuMmmdz_b0xABk5HU82 (accessed on 3 November 2018). (In Portuguese)
19. Morais, M.M.; Novais, M.H.; Penha, A.; Nunes, S.; Morales, E. Avaliação da integridade ecológica de um reservatório na região mediterrânica: Caso de estudo da albufeira do Enxoé, sul de Portugal. *Rev. Ciênc. Tecnol.* **2018**, *2*, 9–25. (In Portuguese)
20. Coelho, H.; Leitão, P.C. Integrated modelling of watersheds and reservoirs. Pocinho and Enxoé cases. *Rev. Bras. Recur. Hídricos.* **2010**, *31*, 77–85.
21. Ramos, T.B.; Gonçalves, M.C.; Branco, M.A.; Brito, D.; Rodrigues, S.; Sánchez-Pérez, J.M.; Sauvage, S.; Prazeres, A.; Martins, J.C.; Fernandes, M.L.; et al. Sediment and nutrient dynamics during storm events in the Enxoé temporary river, southern Portugal. *Catena* **2015**, *127*, 177–190. [CrossRef]
22. Ramos, T.B.; Rodrigues, S.; Branco, M.A.; Prazeres, A.; Brito, D.; Gonçalves, M.C.; Martins, J.C.; Fernandes, M.L.; Pires, F.P. Temporal variability of soil organic carbon transport in the Enxoé agricultural watershed. *Environ. Earth Sci.* **2015**, *73*, 6663–6676. [CrossRef]
23. Brito, D.; Neves, R.; Branco, M.A.; Prazeres, A.; Rodrigues, S.; Gonçalves, M.C.; Ramos, T.B. Assessing water and nutrient long-term dynamics and loads in the Enxoé temporary river basin (southeast Portugal). *Appl. Water Sci.* **2017**, under review.
24. Brito, D.; Neves, R.; Branco, M.C.; Gonçalves, M.C.; Ramos, T.B. Modeling flood dynamics in a temporary river draining to an eutrophic reservoir in southeast Portugal. *Environ. Earth Sci.* **2017**, *76*, 377. [CrossRef]
25. Rodrigues, S.; Ramos, T.B.; Gonçalves, M.C.; Martins, J.C.; Branco, M.A.; Pires, F.P.; Guerreiro, A.; Fernandes, M.L. Erosão hídrica potencial na área da bacia da ribeira do Enxoé. In Proceedings of the Livro de Actas do Encontro Anual da SPCS, INIAV, Oeiras, Portugal, 26–28 June 2013; pp. 57–63. (In Portuguese)
26. Kirkby, M.J.; Irvine, B.J.; Jones, R.J.A.; Govers, G. The PESERA coarse scale erosion model for Europe. I.—Model rationale and implementation. *Eur. J. Soil Sci.* **2008**, *59*, 1293–1306. [CrossRef]
27. Brito, D.; Ramos, T.B.; Gonçalves, M.C.; Morais, M.; Neves, R. Integrated modelling for water quality management in a eutrophic reservoir in south-eastern Portugal. *Environ. Earth Sci.* **2018**, *77*, 40. [CrossRef]
28. Cole, T.M.; Wells, S.A. *CE-QUAL-W2: A Two-Dimensional, Laterally Averaged, Hydrodynamic and Water Quality Model, Version 3.1. User Manual*. U.S.; Army Corps of Engineers: Washington, DC, USA, 2003.
29. European Environment Agency (EEA). The DPSIR framework used by the EEA. Available online: <https://www.eea.europa.eu/help/glossary/eea-glossary> (accessed on 20 May 2018).
30. Skoulidakis, N.Th. The environmental state of rivers in the Balkans—A review within the DPSIR framework. *Sci. Total Environ.* **2009**, *407*, 2501–2516. [CrossRef] [PubMed]
31. Kagalou, I.; Leonardos, I.; Anastasiadou, C.; Neofytou, C. The DPSIR approach for an integrated river management framework. A preliminary application on a Mediterranean site (Kalamas River—NW Greece). *Water Resour. Manag.* **2012**, *26*, 1677–1692. [CrossRef]
32. Vannevel, R. Using DPSIR and Balances to Support Water Governance. *Water* **2018**, *10*, 118. [CrossRef]
33. Jia, Y.Z.; Shen, J.Q.; Wang, H.; Dong, G.G.; Sun, F.H. Evaluation of the Spatiotemporal Variation of Sustainable Utilization of Water Resources: Case Study from Henan Province (China). *Water* **2018**, *10*, 554. [CrossRef]
34. Tscherning, K.; Helming, K.; Krippner, B.; Sieber, S.; Gomez y Paloma, S. Does research applying the DPSIR framework support decision making? *Land Use Policy* **2012**, *29*, 102–110. [CrossRef]
35. Sistema Nacional de Informação de Recursos Hídricos (SNIRH). Sistema Nacional de Informação de Recursos Hídricos. Available online: <http://snirh.apambiente.pt/> (accessed on 15 February 2017).
36. Neitsch, S.L.; Arnold, J.G.; Kiniry, J.R.; Williams, J.R. *Soil and Water Assessment Tool, Theoretical Documentation, Version 2009*; Technical Report, No. 406; Texas Water Resources Institute: College Station, TX, USA, 2011.
37. William, J.R. Sediment routing for agricultural watersheds. *Water Resour. Bull.* **1975**, *11*, 965–974. [CrossRef]

38. Trancoso, A.R.; Braunschweig, F.; Chambel Leitão, P.; Obermann, M.; Neves, R. An advanced modelling tool for simulating complex river systems. *Sci. Total Environ.* **2009**, *407*, 3004–3016. [[CrossRef](#)] [[PubMed](#)]
39. Zalidis, G.C.; Tsiafouli, M.A.; Takavakoglou, V.; Bilas, G.; Misapolinos, N. Selecting agri-environmental indicators to facilitate monitoring and assessment of EU agri-environmental measures effectiveness. *J. Environ. Manag.* **2004**, *70*, 315–321. [[CrossRef](#)] [[PubMed](#)]
40. Torrent, J.; Barberis, E.; Gil-Sotres, F. Agriculture as a source of phosphorus for eutrophication in southern Europe. *Soil Use Manag.* **2007**, *23*, 25–35. [[CrossRef](#)]
41. Withers, P.J.A.; Neal, C.; Jarvie, H.P.; Doody, D.G. Agriculture and eutrophication: Where do we go from here? *Sustainability*. **2014**, *6*, 5853–5875. [[CrossRef](#)]
42. Pinto-Correia, T.; Ribeiro, N.; Sá-Sousa, P. Introducing the montado, the cork and holm oak agroforestry system of Southern Portugal. *Agrofor. Syst.* **2011**, *82*, 99–104. [[CrossRef](#)]
43. Yevenes, M.A.; Mannaerts, C.M. Seasonal and land use impacts on the nitrate budget and export of a mesoscale catchment in Southern Portugal. *Agric. Water Manage.* **2011**, *102*, 54–65. [[CrossRef](#)]
44. Alexandrov, Y.; Laronne, J.B.; Reid, I. Suspended sediment concentration and its variation with water discharge in a dryland ephemeral channel, northern Negev, Israel. *J. Arid Environ.* **2003**, *53*, 73–84. [[CrossRef](#)]
45. Alexandrov, Y.; Laronne, J.B.; Reid, I. Intra-event and inter-seasonal behaviour of suspended sediment in flash floods of the semi-arid northern Negev, Israel. *Geomorphology* **2007**, *85*, 85–97. [[CrossRef](#)]
46. Rovira, A.; Batalla, R.J. Temporal distribution of suspended sediment transport in a Mediterranean basin: The Lower Tordera (NE Spain). *Geomorphology* **2006**, *79*, 58–71. [[CrossRef](#)]
47. de Vente, J.; Poesen, J.; Bazzoffi, P.; van Rompaey, A.; Verstraeten, G. Predicting catchment sediment yield in Mediterranean environments: the importance of sediment sources and connectivity in Italian drainage basins. *Earth Surf. Process. Landf.* **2006**, *31*, 1017–1034. [[CrossRef](#)]
48. Nunes, A.N.; Almeida, A.C.; Coelho, C.O.A. Impacts of land use and cover type on runoff and soil erosion in a marginal area of Portugal. *Appl. Geogr.* **2011**, *31*, 687–699. [[CrossRef](#)]
49. Huber, S.; Prokop, G.; Arrouays, D.; Banko, G.; Bispo, A.; Jones, R.J.A.; Kibblewhite, M.; Lexer, W.; Moller, A.; Rickson, R.J.; et al. *Environmental Assessment of Soil for Monitoring: Volume I Indicators & Criteria*; Office for the Official Publications of the European Communities: Luxembourg City, Luxembourg, 2008; p. 339.
50. Boix-Fayos, C.; Martínez-Mena, M.; Arnau-Rosalén, E.; Calvo-Cases, A.; Castillo, V.; Albaladejo, J. Measuring soil erosion by field plots: Understanding the sources of variation. *Earth Sci. Rev.* **2006**, *78*, 267–285. [[CrossRef](#)]
51. Cammeraat, E.L.H. A review of two strongly contrasting geomorphological systems within the context of scale. *Earth Surf. Process. Landf.* **2002**, *27*, 1201–1222. [[CrossRef](#)]
52. Cammeraat, E.L.H. Scale dependent thresholds in hydrological and erosion response of a semi-arid catchment in Southeast Spain. *Agric. Ecosys. Environ.* **2004**, *104*, 317–332. [[CrossRef](#)]
53. Osterkamp, W.R.; Toy, T.J. Geomorphic considerations for erosion prediction. *Environ. Geo.* **1997**, *29*, 152–157. [[CrossRef](#)]
54. Bull, L.J. Magnitude and variation in the contribution of bank erosion to the suspended sediment load of the River Severn, UK. *Earth Surf. Process. Landf.* **1997**, *22*, 1109–1123. [[CrossRef](#)]
55. Lefrançois, J.; Grimaldi, C.; Gascuel-Oudou, C.; Gilliet, N. Suspended sediment and discharge relationships to identify bank degradation as a main sediment source on small agricultural catchments. *Hydrol. Process.* **2007**, *21*, 2923–2933. [[CrossRef](#)]
56. Butturini, A.; Gallart, F.; Latron, J. Cross-site comparison of variability of DOC and nitrate C–Q hysteresis during the autumn–winter period in three Mediterranean headwater streams: A synthetic approach. *Biogeochemistry* **2006**, *77*, 327–349.
57. Walling, D.A.; Webb, B.W. *Erosion and Sediment Yield: A Global Overview*; IAHS Press: Oxford, England, 1996; pp. 3–19.
58. Casali, J.; Giménez, R.; Díez, J.; Álvarez-Mozos, J.; Del Valle de Lersundi, J.; Goñi, M.; Campo, M.A.; Chahor, Y.; Gastesi, R.; López, J. Sediment production and water quality of watersheds with contrasting land use in Navarre (Spain). *Agric. Water Manage.* **2010**, *97*, 1683–1694. [[CrossRef](#)]
59. Oeurng, C.; Sauvage, S.; Sanchez-Pérez, J.M. Assessment of hydrology, sediment and particulate organic carbon yield in a large agricultural catchment using the SWAT model. *J. Hydrol.* **2011**, *401*, 145–153. [[CrossRef](#)]

60. Strohmeier, S.; Knorr, K.H.; Reichert, M. Concentrations and fluxes of dissolved organic carbon in runoff from a forested catchment: Insights from high frequency measurements. *Biogeosci. Disc.* **2013**, *10*, 905–916. [[CrossRef](#)]
61. Havens, K.E.; James, R.T.; East, T.L.; Smith, V.H. N:P ratios, light limitation and cyanobacterial dominance in a subtropical lake impacted by non-point source nutrient pollution. *Environ. Poll.* **2003**, *122*, 379–390. [[CrossRef](#)]
62. Søndergaard, M.; Jensen, J.P.; Jeppesen, E. Role of sediment and internal loading of phosphorus in shallow lakes. *Hydrobiologia* **2003**, *506*, 135–145. [[CrossRef](#)]
63. Jarvie, H.P.; Sharpley, A.N.; Withers, P.J.A.; Scott, J.T.; Haggard, B.E.; Neal, C. Phosphorus mitigation to control river eutrophication: Murky waters, inconvenient truths, and “postnormal” science. *J. Environ. Qual.* **2013**, *42*, 295–304. [[CrossRef](#)] [[PubMed](#)]



© 2018 by the authors. Licensee MDPI, Basel, Switzerland. This article is an open access article distributed under the terms and conditions of the Creative Commons Attribution (CC BY) license (<http://creativecommons.org/licenses/by/4.0/>).